# Continuous Flow Characterization of Solid Biomass in a Reciprocating/Rotating Scraper Tube: An Experimental Study

**Kamelia V. K. Boodhoo and Lily Smith**
School of Chemical Engineering and Advanced Materials, Merz Court, Newcastle University, Newcastle Upon Tyne, NE1 7RU, U.K.

**Juan Pedro Solano**
Dept. Ingeniería Térmica y de Fluidos, Universidad Politécnica de Cartagena, Campus Muralla del Mar s/n, Cartagena 30202, Spain

**Mark Gronnow and James Clark**
Green Chemistry Centre of Excellence, Dept. of Chemistry, University of York, York, YO10 5DD, U.K.

*DOI 10.1002/aic.14571*
*Published online August 11, 2014 in Wiley Online Library (wileyonlinelibrary.com)*

*The performance of reciprocating/rotating scrapers has been assessed in a visualization study of the continuous flow hydrodynamics of air-fluidized solid biomass under varying conditions of air flow rate and scraping velocities. A combination of low air flow rates and high scraping velocities results in more uniform flow of both types of biomass investigated. Power consumed by the reciprocating action of the scrapers increases with the scraping velocity but typically represents no more than 20% of the overall power consumption at the highest air flow rate applied. We also demonstrate that rotation of the scrapers superimposed on their reciprocating action gives higher flow rate of biomass and better mixing within the bulk solid compared to reciprocating action alone. The application of the reciprocating/rotating scraper technology described in this study represents a viable step forward in developing a continuous, large-scale process for the microwave-assisted decomposition of solid biomass to produce bio-oils.* © 2014 American Institute of Chemical Engineers *AIChE J*, 60: 3732–3738, 2014

*Keywords: gas–solid multiphase flow, horizontal tubular reactor, reciprocating/rotating scrapers, solid biomass, fluidization*

## Introduction

The use of sustainable sources of carbon has been identified as one of the major promising routes to a low carbon solution in the replacement of the use of fossil resources. Andrews and Jelley[1] suggest that biomass represents the only viable renewable source for carbon-based fuels and chemicals and is a low carbon solution for the future global energy supply. Conventional pyrolysis is one of the oldest biomass processing technologies[2] which produces bio-gas, bio-oils, and char, and where the biomass is thermally treated in electric or gas furnaces across a range of temperatures between 200°C and 600°C under inert, atmospheric conditions. However, these methods do not favor the conversion to bio-oil and have many drawbacks such as poor heat transfer rates and major heat losses to the surroundings and undesired secondary reactions due to the high residence times in a high temperature environment. As an alternative to conventional pyrolysis, microwave activation of solid biomass has been shown to be a promising novel, energy efficient route to bio-oils[2–9] which results in more rapid and controllable heating rates of the solid biomass.

Much of the previous work on conversion of solid biomass by microwave has been performed in conventional batch vessels which are acceptable for small scale processing. However, economic and viable commercial scale conversion technologies exploiting microwave technology will require the development of continuous processing technologies for solid displacement. There are numerous examples of continuous flow tubular or coil reactors which have been developed for microwave heating applications[10,11] but these have been designed primarily with liquid phase processes in mind, although the formation of metal nanoparticles in such systems have also been reported.[12]

Gas–solid fluidized bed reactors for high temperature pyrolysis of solid biomass to produce bio-oils are commonly used.[8,13,14] Such fluidized bed reactors are generally in the form of an empty tube through which solid biomass is continuously fed by screw feeding[14,15] and its residence time is typically of the order of a few seconds. However, these designs would not be suitable for microwave processing applications reported to require higher residence times of up to 10 min in batch processes to achieve reasonable yields.[2]

Additional Supporting Information may be found in the online version of this article.

Correspondence concerning this article should be addressed to K. V. K. Boodhoo at kamelia.boodhoo@ncl.ac.uk.

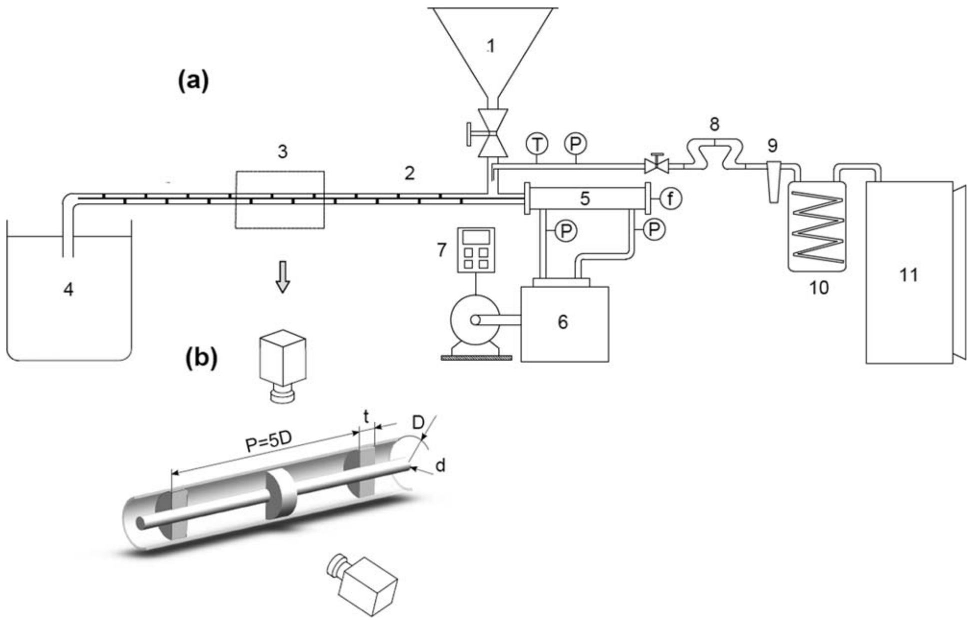


**Figure 1. (a) Experimental rig (b) geometry of the tube scraper and definition of visualization planes.**

We focus our attention in this study on the application of a variant of the empty tube fluidized bed reactors which involves reciprocating/rotating scraper technology to aid the continuous flow of solid biomass. Rotating and reciprocating scrapers have conventionally been applied in heat exchangers, particularly for viscous liquids.[16–20] The work of Solano and coworkers[17–20] is particularly relevant as they investigated a scraped surface heat exchanger that utilizes a reciprocating motion with and without rotation. The reciprocating scrapers are illustrated schematically in Figure 1b, whereby an array of semicircular elements are mounted onto a rod with a pitch $P = 5D$. These semicircular elements fit inside the tube such that, when in reciprocating motion, the elements scrape the inside wall to displace material and eliminate fouling. As well as improving the heat transfer at the wall of the heat exchanger it was observed that the addition of the reciprocating motion generates macroscopic displacements of the flow, improving mixing within the heat exchanger. This feature is very relevant for the potential application involving solid biomass activation by microwaves, as the uniform exposure of all the biomass surfaces to the microwave energy would be key in achieving good overall decomposition rates.

The present investigation looks into the applicability of the reciprocating/rotating scraper technology for solid-gas multiphase flow primarily in the turbulent regime. If this technology proves to be promising, it could be developed further as a continuous flow reactor system for the microwave-assisted decomposition of solid biomass to produce bio-oils.

## Materials and Methods

A schematic diagram of the rig set up is shown in Figure 1a. The reciprocating scraper device shown in Figure 1b was inserted into a transparent Perspex tube (2) of inner diameter $D = 74$ mm and 1.8-m long. The scrapers were mounted on a central rod of diameter $d = 18$ mm at a pitch $P$ of 370 mm. The reciprocating motion of the scrapers was provided by a hydraulic piston (5). The dimensions and characteristics of the pistons used in this study are given in Table 1. The hydraulic unit (6) comprised an oil tank, the pump and a 4-way valve. A frequency converter (7) was used to regulate the pump rotational speed. The biomass was stored in a feed tank (1) above the entrance of the reaction tube and was fed into the tube via gravity. The feed tank, designed to hold up to approximately 30 L of material, was fitted with a lid to alleviate the back pressure in the feed tank. A thick layer of Teflon between the tank and the lid which was fixed into position by metal clamps ensured that no air can escape from the top end of the feed vessel. The flow of biomass from the feed tank into the reciprocating tube was manipulated manually by a ball valve. The biomass was pneumatically conveyed through the tube suspended in air which is provided by a compressor (11). The air was passed through a dehumidifier (10) and a filter (9) to remove any moisture and impurities before the flow rate was measured by a Coriolis flow meter (8) (Micromotion model with a range of 0–500 kg/h). A hand operated ball valve allowed the air flow rate into the tube to be varied and its temperature was measured using a T-type thermocouple. The spent biomass was directed through a plastic tube into a bin (3) attached to the end of the reaction tube.

Parameters of interest in this study were: biomass type, air flow rate, and scraper velocity. Two distinct types of biomass were used: (1) wood pellet density of 1.1 g/cm$^3$, 5 mm diameter, and 10–20 mm long and (2) milled barley straw density of 0.117 g/cm$^3$, 1 mm diameter, and 1–5 mm long (Figures 2a, b respectively). Table 2 gives the range of parametric conditions that were explored for each type of biomass.

Visual observations are presented in this study of the flow patterns which have been video recorded using a high speed

**Table 1. Piston Dimensions and Operating Capability**

| | Piston 1 | Piston 2 |
|---|---|---|
| Scraping periods | Stationary, 10 s, 5 s | 2.5 s, 1 s |
| Chamber diameter, $D_c$ | 50 mm | 24.9 mm |
| Piston diameter, $D_p$ | 20 mm | 18 mm |
| Stroke, $S$ | 180 mm | 175 mm |

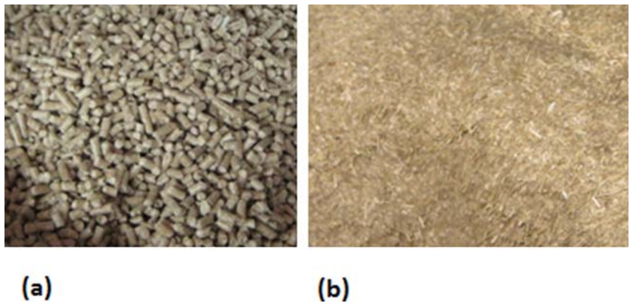


**Figure 2. (a) Wood pellet biomass (b) milled straw biomass.**

[Color figure can be viewed in the online issue, which is available at wileyonlinelibrary.com.]

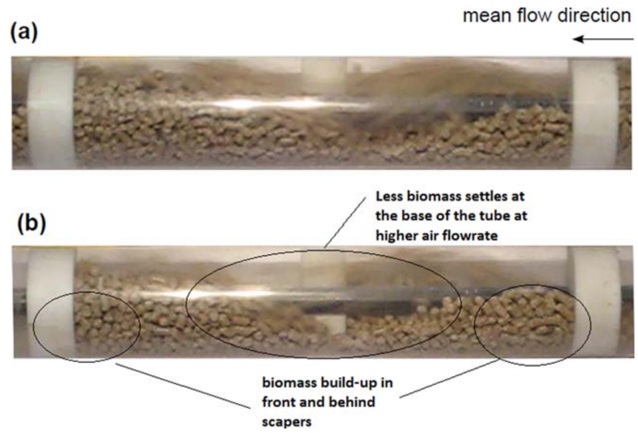


**Figure 3. Flow of wood pellet biomass (a) air flow rate 90 kg/h (*Re* = 20000) and stationary scrapers (b) air flow rate of 110 kg/h (*Re* = 24000) and stationary scrapers.**

[Color figure can be viewed in the online issue, which is available at wileyonlinelibrary.com.]

camera positioned above the flow tube and a digital camera positioned to the side of the tube, as shown in Figure 1b.

## Results and Discussion

### *Effect of air flow rate*

*Wood Pellet Biomass.* The effect of air flow rate on the flow patterns exhibited by the wood pellets is depicted in Figures 3a, b where the solid biomass flows from right to left. Two distinct flow patterns are evident: there is a fast flowing phase that is suspended in the air flow at the top of the tube and a slow moving bulk phase at the bottom of the tube between successive scraper plugs. The bulk phase is heavily affected both by gravity and the presence of the scraper plugs. Without any reciprocating scraper motion, there is no movement of the biomass at the bottom of the bulk phase at all. Although the scraping plugs are themselves obstacles to the flow, the two flow phases would not be eliminated even if the plugs were removed. Rather, in the absence of the plugs, the phases would not be as distinct and a more gradual velocity profile would be observed along the vertical plane of the tube.

The build up of the bulk biomass phase occurs behind and in front of the scraper plugs. This is more evident at higher air flow rates (Figure 3b) where a larger amount of the biomass is in the suspended phase and vacates a larger volume of the tube. At lower air flow rates the biomass builds up in the whole section between the scraper plugs leaving a smaller amount of biomass in the suspended phase (Video 1 in the Supporting Information).

The suspended phase consists of a small amount of biomass that is carried along the length of the tube, suspended in the air. Figure 4 and Supporting Information Video 2 illustrate the flow pattern of the suspended biomass phase in the air stream. The picture is taken directly above the tube, and therefore, shows the flow pattern in the horizontal plane.

**Table 2. Range of Operating Conditions**

| | Wood Pellets | Milled Straw |
|---|---|---|
| Air flow rate (kg/h) | 90, 110, 135, and 160 | 10, 20, and 30 |
| Scraping periods of reciprocating scrapers (using Piston 1) | 5 s, 10 s, and stationary scrapers | 5 s, 10 s, and stationary scrapers |
| Scraping periods of reciprocating scrapers (using Piston 2) | 2.5 s, 1 s[a] | 2.5 s, 1 s[b] |

[a]Air flow rate tested was limited to 90 kg/h.
[b]Air flow rate tested was limited to 10 kg/h.

The suspended biomass follows a meandering path through the tube avoiding the scraper plugs, as illustrated by the arrows. This flow pattern is more prominent at lower air flow rates; as the air flow rate is increased, the biomass tends to collide with the scraper plugs to a greater extent and to disintegrate as a result. This observation may be explained by the wood pellets having a high Stokes number (typically two orders of magnitude higher than the milled straw biomass) due to their relatively large particle size and high density so that they are less prone to follow the trajectory of the air flow and to avoid collisions with obstacles along the way.

As the air flow rate increases, it is observed that the ratio of the suspended biomass to the bulk biomass increase. At a certain air flow rate, the bulk biomass phase ceases to exist and the full flow of biomass is in suspension. For the wood pellet biomass, this occurs at an air flow rate of around 160 kg/h.

*Milled Straw Biomass.* The flow pattern of the milled straw biomass is comparable to the wood pellet biomass. As seen in Figure 5 and Supporting Information Video 3, the milled straw biomass exhibits the two distinct flow phases also observed with the wood pellet biomass. Generally, the flow of the milled straw biomass in the tube is observed to be less uniform than the wood pellets due to the milled straw particles forming bridges and adhering to the walls of the feed tank upstream of the tube. Figures 5a, b highlight that at the highest air flow rate of 30 kg/h, there is less of the milled straw settling at the base of the tube. The investigation has not been extended to include even higher air flow rates that would ensure that all the milled straw would be in the suspended phase. At such a high air flow rate, the biomass flow rate would be very high, resulting in a very short

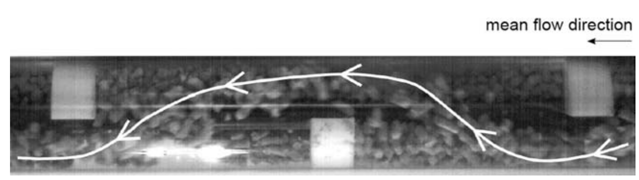


**Figure 4. Suspended phase flow pattern for wood pellet biomass: top view.**

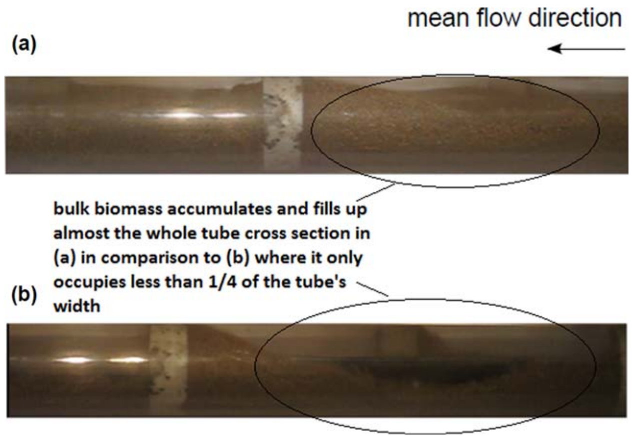


**Figure 5. Flow of milled straw biomass (a) air flow rate 10 kg/h ($Re = 2200$) and stationary scrapers (b) air flow rate 30 kg/h ($Re = 6600$) and stationary scrapers.**

[Color figure can be viewed in the online issue, which is available at wileyonlinelibrary.com.]

residence time in the tube, which may not be desirable for the proposed application of microwave decomposition of solid biomass.

### *Effect of scraping velocity*

Figures 6a, b illustrate still shots of the wood pellet biomass flow when subjected to an air flow rate of 90 kg/h at 10 s and 1 s scraping period, respectively. The corresponding video shots are shown in Supporting Information Video 4.

Visual analysis of the animations suggests that higher scraping velocities provide enhanced mixing of the biomass. A transitional phase develops obscuring the discrete divide between the bulk and suspended phases. This occurs to a greater extent at higher scraping velocities. Increasingly more rapid mixing of the biomass within the tube leads to a greater amount of biomass being picked up by the air flow, hence increasing the biomass flow rate. The reciprocating movement of the scrapers helps to reduce the dead spots that appear near the scraper plugs. A build up of biomass can nevertheless still be observed in front of and behind the scraper plugs. However, the biomass particles are constantly being renewed and the rate at which the biomass particles are replaced increases with scraping velocity.

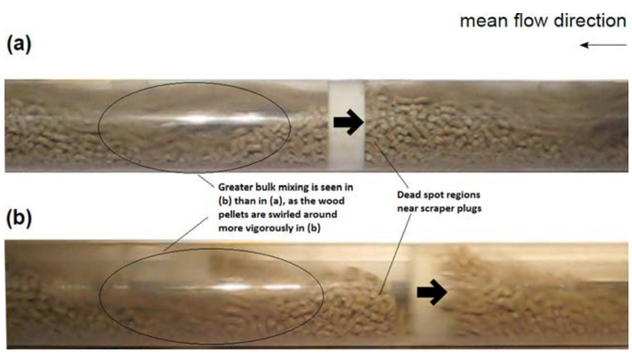


**Figure 6. Effect of scraping velocity on wood pellet biomass, air flow rate 90 kg/h (a) 10 s scraping period (b) 1 s scraping period. (The thick arrows on the scrapers indicate the direction of their movement)**

[Color figure can be viewed in the online issue, which is available at wileyonlinelibrary.com.]

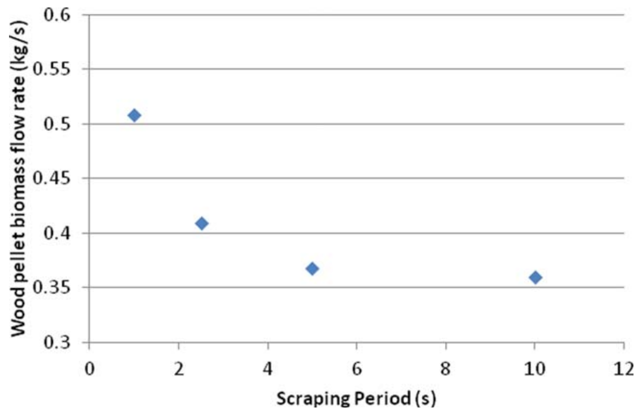


**Figure 7. Effect of scraping period on wood pellet biomass flow rate with an air flow rate of 90 kg/h.**

[Color figure can be viewed in the online issue, which is available at wileyonlinelibrary.com.]

Another observation more readily observable from Supporting Information Video 4, especially at the highest scraper velocity (corresponding to scraping period of 1 s), is that the flow pattern and mixing differ depending on whether the scrapers are in co-current or counter-current motion with the air flow. When the scraper plugs move in the same direction as the net flow of biomass, the suspended biomass phase follows the previously observed meandering path between the scrapers. The bulk biomass is pushed forward along the tube by the scraper plugs at the same velocity as the reciprocating motion. Conversely, when the scraper plugs move in the opposite direction to the net flow of the biomass, greater movement of the bulk biomass is forced. As the scraper initially moves backward a gap is formed in front of the scraper plug which is filled, at the base of the tube, by the biomass from behind the scraper plug on opposite side of tube. As the scraper plug continues to move further backward, the air flow and friction of the tube apply opposing forces to the plug, which cause the biomass to move upward around the outside of the tube as well as moving in a forward motion, following a helical path around the outside of the tube.

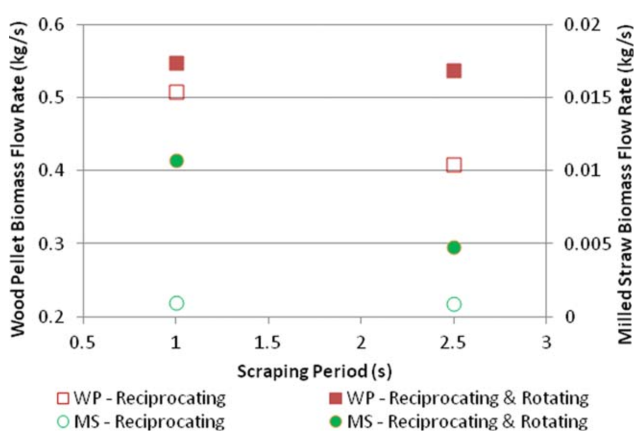


**Figure 8. Effect of rotating scrapers on biomass flow rate. (WP: wood pellets; MS: milled straw)**

[Color figure can be viewed in the online issue, which is available at wileyonlinelibrary.com.]

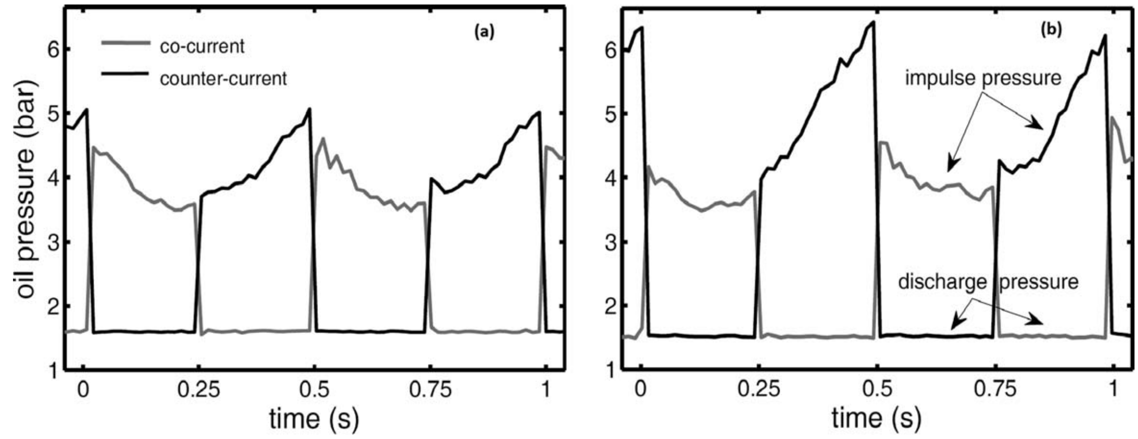


**Figure 9. Pressure signal for scraping period of 5 s using wood pellet biomass (a) air flow rate 90 kg/h (b) air flow rate 160 kg/h.**

The suspended flow of wood pellets is observed to be less concentrated in the air stream at lower scraper velocities represented by longer scraping periods. This observation is further validated by the suspended biomass flow rate measured under various scraping periods as shown in Figure 7.

The scraping period appears not to have as much effect on the bulk mixing of the milled straw biomass compared with the wood pellet biomass. This could be due to the smaller size of the milled straw particles when compared to the diameter of the tube resulting in them being more tightly packed. Although increasing the scraping velocity does not appear to enhance the mixing within the bulk of the milled straw, its overall displacement through the tube is enhanced. When the scrapers are stationary, the bulk biomass occupies more than three quarters of the tube volume between the scrapers and its profile is quite flat. There appears to be hardly any net flow in the bulk phase. Under reciprocating motion, however, although there is a build up of biomass behind and in front of the scraper plugs, the level of biomass resting between two consecutive scraper plugs decreases as the scraping velocity increases. This indicates that, in spite of the reduced bulk mixing, the higher velocity of the reciprocating action is nevertheless able to shift the milled straw biomass more effectively along the tube.

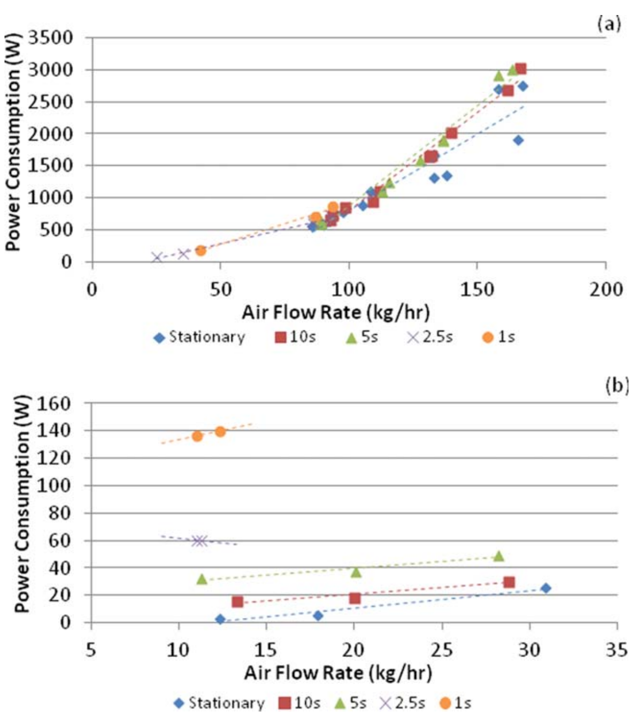


**Figure 10. Overall power consumption at various scraping periods and air flow rates (a) wood pellets (b) milled straw.**

**[Color figure can be viewed in the online issue, which is available at wileyonlinelibrary.com.]**

*Rotating Scrapers.* It is observed that enhanced mixing of the biomass and an increase in net flow is generated when rotating motion of the scrapers is superimposed on the reciprocating action (Supporting Information Video 5). During the rotating motion, the scrapers also act as tool to break up the bulk biomass which would otherwise settle at the base of the tube. This effect can be seen in Figure 8, in which the flow rates of biomass are shown to increase when the scraping device is rotated as well as reciprocated at two scraping periods, 1 and 2.5 s. The wood pellet biomass flow rate increases slightly at the 1 s scraping period by a factor of 1.08 and at the 2.5 s scraping period the increase is by a factor of 1.32. It can be seen that the rotation of the scrapers has a much greater effect on the milled straw biomass flow rate which increases by factors of 5.5 and 10 for the 2.5 and 1 s scraping periods, respectively.

### *Power consumption*

The power consumption of the system is made up of two parts: the power required by the piston to move the scrapers and the power required to pump the air. As described by Solano et al.,[20] the power consumption of the scrapers is obtained by measuring the oil pressure, which is time dependent, in both chambers of the hydraulic piston. It is expressed in Eq. 1 in terms of the operating characteristics of the piston

$$\mathrm{Power}_{\mathrm{scr}} = \left(\frac{\pi\left(D_{\mathrm{c}}^2 - D_{\mathrm{p}}^2\right)}{4}\right) S \frac{\Delta P_{\mathrm{scr}}}{\Delta t/2} \tag{1}$$

where the scraping period $\Delta t$ (s), is measured by a timing device connected to final-stroke switches which constrain the scraping stroke $S$ (backward or forward) to the value $S = P$ (370 mm).

Figure 9 illustrates the signal obtained from the pressure sensors on the hydraulic piston during two typical operating regimes. The scraper moves in the same direction as the net fluid flow during the cocurrent half-cycle, conversely the scraper moves in the opposite direction to the net fluid flow during the countercurrent half-cycle. The impulse pressure (see Figure 9b) is the pressure of the oil that is being diverted to the corresponding piston chamber. The discharge pressure is the pressure in the other chamber that is being discharged. The average pressure difference, $(\Delta P)_{\mathrm{scr}}$, between the impulse pressure and the discharge pressure is used in Eq. 1 to calculate the power consumed by the piston. Different power consumption values are measured during the co-current and counter-current half-cycles; therefore, the power consumed by the scraper is the average of the two.

The power required to pump the air through the system can be described by Eq. 2

$$\mathrm{Power}_{\mathrm{a}} = \frac{m \Delta P_{\mathrm{a}}}{\rho} \tag{2}$$

where the mass flow rate, $m$, is measured via a coriolis flow meter.

The overall power consumption is, therefore, given as

$$\mathrm{Power} = \left( \frac{\pi \left( D_{\mathrm{c}}^2 - D_{\mathrm{p}}^2 \right)}{4} \right) S \cdot \frac{\Delta P_{\mathrm{scr}}}{\Delta t / 2} + \frac{m \Delta P_{\mathrm{a}}}{\rho} \tag{3}$$

Figures 9a, b highlight the difference in the measured pressure at different air flow rates with the scraping period held constant at 5 s. Although the oil pressure recorded under co-current motion is similar for both cases, the oil pressure under counter-current motion is increased when the air flow rate is higher. This higher pressure that is required to move the scraper plugs in the counter-current motion accounts for an increased scraping power required at higher air flow rates. It is to be noted that, especially for the wood pellet biomass where high air flow rates are used, the scraping power typically represents no more than 20% of the overall power consumed.

The power consumption of the system when subjected to changing air flow rate and scraping period is illustrated in Figures 10a, b for the wood pellets and for milled straw, respectively. It can be seen that for a given scraping period the power consumption generally increases as the air flow rate increases, as expected, except for one set of anomalous result for the 2.5 s scraping period using the milled straw which is attributed to an error in the measured air flow rate. Furthermore, for any fixed air flow rate, the power consumption of the process generally increases as the scraping period decreases. It is worth noting that the overall power consumed for the wood pellets shown in Figure 10a is an order of magnitude higher than for the milled straw due to the much higher air flow rates used, and the relative scraper power increases at higher scraper velocities are thus proportionally smaller than those of the milled straw in Figure 10b. At the lower scraping period, the velocity of the reciprocating scraper is greater, causing increased friction between the scraper plugs and inner wall of the tube. This increased resistance is overcome by the higher oil pressures in the piston chambers, which results in more power being consumed.

## Conclusions

In this work, the feasibility of reciprocating/rotating scraper technology combined with pneumatic conveying as a continuous transportation method for two types of solid biomass of different densities has been investigated.

Without the reciprocating motion of the scrapers, the biomass exhibits two discrete flow phases, a slow moving bulk phase that travels across the base of the tube and a faster moving suspended phase. Low air flow rates and high scraping velocities have been identified as providing the optimum conditions for the two types of biomass using the scrapers in reciprocating mode. The air flow rates are 90 and 10 kg/h for wood pellet biomass and milled straw biomass, respectively, both generating best displacement conditions at a 1 s scraping period. Higher scraping velocity (represented by shorter scraping periods) of the reciprocating scrapers also results in better mixing within the bulk of the wooden pellets where as little mixing improvement is observed with scraping velocity for the milled straw. Dead spots that tend to form next to the scraper plugs are nevertheless greatly reduced at higher scraping velocities. Scraping power which increases with scraper velocity typically represents no higher than 20% of the overall power consumed at the highest flow rates of 160 kg/h using the wood pellets.

Rotation of the reciprocating scrapers demonstrates a distinct potential to further enhance mixing of the biomass. A combination of rotation and reciprocating movement is more beneficial in aiding the flow of the solid biomass as demonstrated by the higher flow rates of displaced biomass under these conditions.

It is envisaged that this technology could be a step forward in developing a continuous, large-scale process for the microwave-assisted decomposition of solid biomass to produce bio-oils. The ability of the moving scrapers to clean the inner surface of the tube while aiding the displacement and mixing of the solid biomass during its exposure to the microwave energy field is an important advantage if viscous oils are formed and deposited on the tube walls. Further design considerations concerning the *in situ* separation of the oil from the solid biomass residue as it flows through the tube would need to be explored and implemented for operation in this particular application.


## Acknowledgment

The authors gratefully acknowledge Dr. J. Pérez, Dr. P.G. Vicente, and Mr D.S. Martínez for their unselfish contribution to build the experimental facility and for their valuable help and advice.


## Notation

d = rod diameter, m
$D$ = inner tube diameter, m
$D_{\mathrm{c}}$ = piston chamber diameter, m
$D_{\mathrm{h}}$ = hydraulic diameter of tube, (= $D$–$d$), m
$D_{\mathrm{p}}$ = piston diameter, m
$m$ = mass flow rate, kg/s
$P$ = scraper pitch or pressure, m or bar
$\Delta P$ = pressure drop or pressure difference, bar
$S$ = stroke, m
$\Delta t$ = scraping period, s
$V$ = velocity, m/s

### *Greek letters*

$\mu$ = dynamic viscosity, Pa.s
$\rho$ = density, kg/m$^3$

### *Dimensionless groups*

$Re$ = Reynolds number, = $\rho V D_{\mathrm{h}}/\mu$

### *Subscripts*

a = air
scr = scraper

## Literature Cited


1. Andrews J, Jelley N. *Energy science: principles, technologies and impacts*. Oxford: Oxford University Press, 2007.
2. Budarin VL, Clark JH, Lanigan BA, Shuttleworth P, Breeden SW, Wilson AJ, Macquarrie DJ, Milkowski K, Jones J, Bridgeman T, Ross TA. The preparation of high-grade bio-oils through the controlled, low temperature microwave activation of wheat straw. *Bioresour Technol*. 2009;100:6064–6068.
3. Budarin VL, Clark JH, Lanigan BA, Shuttleworth P, Macquarrie DJ. Microwave assisted decomposition of cellulose: a new thermochemical route for biomass exploitation. *Bioresour Technol*. 2010;101:3776–3779.
4. Wan Y, Chen P, Zhang B, Yang C, Liu Y, Lin X, Ruan R. Microwave-assisted pyrolysis of biomass: catalysts to improve product selectivity. *J Anal Appl Pyrolysis*. 2009;86:161–167.
5. Wang X, Chen H, Luo K, Shao J, Yang H. The influence of microwave drying on biomass pyrolysis. *Energy Fuels*. 2008;22:67–74.
6. Gronnow MJ, White RJ, Clark JH, Macquarrie DJ. Energy efficiency in chemical reactions: a comparative study of different reaction techniques. *Org Process Res Dev*. 2005;9:516–518.
7. Miura M, Kaga H, Sakurai A, Kakuchi T, Takahashi K. Rapid pyrolysis of wood block by microwave heating. *J Anal Appl Pyrolysis*. 2004;71:187–199.
8. Mohan D, Pittman CU, Steele PH. Pyrolysis of wood/biomass for bio-oil: a critical review. *Energy Fuels*. 2006;20:848–889.
9. Tian Y, Zuo W, Ren Z, Chen D. Estimation of a novel method to produce bio-oil from sewage sludge by microwave pyrolysis with the consideration of efficiency and safety. *Bioresour Technol*. 2011;102:2053–2061.
10. Encinar JM, González JF, Martínez G, Sánchez N, Pardal A. Soybean oil transesterification by the use of a microwave flow system. *Fuel*. 2012;95:386–393.
11. Wegner J, Ceylan S, Kirschninga A. Flow chemistry—a key enabling technology for (multistep) organic synthesis. *Adv Synth Catal*. 2012;354:17–57.
12. Dzido G, Jarzebski AB. Fabrication of silver nanoparticles in a continuous flow, low temperature microwave-assisted polyol process. *J Nanopart Res*. 2011;13:2533–2541.
13. Bridgwater AV. Renewable fuels and chemicals by thermal processing of biomass. *Chem Eng J*. 2003;91:87–102.
14. DeSisto WJ, Hill N, Beis SH, Mukkamala S, Joseph J, Baker C, Ong TH, Stemmler EA, Wheeler MC, Frederick BG, van Heiningen A. Fast pyrolysis of pine sawdust in a fluidized-bed reactor. *Energy Fuels*. 2010;24:2642–2651.
15. Salehi E, Abedi J, Harding T. Bio-oil from sawdust: effect of operating parameters on the yield and quality of pyrolysis products. *Energy Fuels*. 2011;25:4145–4154.
16. Rao CS, Hartel RW. Scraped Surface Heat Exchangers. *Crit Rev Food Sci Nutr*. 2006;46:207–219.
17. Solano JP, García A, Vicente PG, Viedma A. Flow field and heat transfer investigation in tubes of heat exchangers with motionless scrapers. *Appl Therm Eng*. 2011;31:2013–2024.
18. Martínez DS, Solano JP, Pérez J, Viedma A. Numerical investigation of non-Newtonian flow and heat transfer in tubes of heat exchangers with reciprocating insert devices. *Front Heat Mass Trans*. 2011;2:1–10.
19. Solano JP, García A, Vicente PG, Viedma A. Flow pattern assessment in tubes of reciprocating scraped surface heat exchangers. *Int J Therm Sci*. 2010;50:803–815.
20. Solano JP, García A, Vicente PG, Viedma A, Performance evaluation of a zero-fouling reciprocating scraped-surface heat exchanger. *Heat Trans Eng*. 2011;32:331–338.


*Manuscript received Apr. 7, 2014, and revision received June 26, 2014.*